scientific reports

Check for updates

OPEN

Potassium dichromate induces dose-dependent nephrotoxicity through oxidative stress-mediated downregulation of renal aquaporins and upregulation of KIM-1

Hossam Shehab[1], Ibrahim El Tantawy El Sayed[1], Eman A. Badr[2,3], Nuha Anajirih[4], Afaf Abdelkader[5], Eman E. ELwakeel[6,7], Nagah E. Ali[5], Enas M. Kasem[8], Fatma Al-Zahraa N. Al-Shahed[9], Madaniah O. Zakari[10], Ekramy M. Elmorsy[11], Samah F. Ibrahim[12], Mustafa Shukry[13]✉, Eman M. El Nashar[14], Areej M. Alshehri[15], Ahmad F. Rawan[16]✉ & Ahmed Abdeen[17,18]✉

Potassium dichromate (Cr) is a ubiquitous inorganic chemical reagent, most frequently employed as an oxidizing agent in variety of laboratory and industrial settings and can result in nephrotoxicity. The current study was done to explore the nephrotoxic effects of Cr with a specific focus on alterations in renal aquaporins (AQPs) expression, renal water channel protein, providing insights into how exposure to Cr may compromise renal water homeostasis in a dose-dependent pattern. Thirty-six Wistar albino male rats were assigned into 3 groups evenly; control rats received only distilled water daily, while Cr-Low and Cr-High groups received, 2.5 mg/kg bw, and 7.5 mg/kg bw of Cr i.p for 14 days, respectively. Blood and kidney samples were obtained. Cr induced nephrotoxicity in the current study in a dose-dependent manner, as exhibited by a remarkable deterioration of the renal parameters, oxidative status, histopathological and ultrastructural changes. Renal function registered a significant rise in urea and creatinine, as opposed to total protein and albumin, which decreased substantially. A significant dose dependent rise in malondialdehyde (MDA) level as well as dwindle in the antioxidant enzymes level. Furthermore, hematology divulged a notable reduction in hemoglobin concentration (Hb%) while significant upsurge in white blood cells (WBCs) in exposed groups. In addition, our study demonstrated that Cr, alters the expression level of AQP1 and AQP2 in renal tissue which are salutary for detecting the renal damage early. On the other hand, Cr boosted the upregulation of kidney injury molecule-1 (KIM-1) in kidney tissue confirming its disruption. Interestingly, gene expression of KIM-1, AQP1 and AQP2's in renal membrane correlates well with creatine level, reinforcing their role as sensitive markers of tubular damage and reflect impaired tubular water handling. High exposure produced a severe nephrotoxic profile, distinctly different from controls and far more pronounced than the Cr-Low group.

Keywords Nephrotoxicity, Potassium dichromate, Oxidative stress, Aquaporins, KIM-1, Dose-dependent

[1]Department of Chemistry, Faculty of Science, Menoufia University, Shebin El- Koom 13829, Egypt. [2]Department of Medical Biochemistry and Molecular Biology, Faculty of Medicine, Menoufia University, Shebin El-Koom 13829, Egypt. [3]Department of Biochemistry and Molecular Biology, Faculty of Applied Health Science technology, Menoufia National University, Menoufia, Egypt. [4]Department of Emergency Medical Services, Faculty of Health Sciences, Al Qunfudhah, Umm Al-Qura University, 21912 Makkah, Saudi Arabia. [5]Department of Forensic Medicine and Clinical Toxicology, Faculty of Medicine, Benha University, Benha 13518, Egypt. [6]Department of Anatomy and Embryology, Faculty of Medicine, Benha University, Benha 13518, Egypt. [7]Department of Basic Science, Faculty of Nursing, Riyadh Elm University, Riyadh, Saudi Arabia. [8]Department of Physiology, Faculty of Medicine, Benha University, Benha 13518, Egypt. [9]Department of Histology and Cell Biology, Faculty of Medicine, Al-Azhar University, Cairo, Egypt. [10]Department of Basic Medical Sciences, College of Medicine, Taibah University, Medina 41477, Saudi Arabia. [11]Center for Health Research, Northern Border University, Arar 91431, Saudi Arabia. [12]Department of Internal Medicine, College of Medicine, Princess Nourah bint Abdulrahman University, P.O. Box

84428, Riyadh 11671, Saudi Arabia. [13]Department of Biomedical Sciences, College of Veterinary Medicine, King Faisal University, Saudi Arabia, P.O. Box 400, Al-Ahsa 31982, Saudi Arabia. [14]Department of Anatomy, College of Medicine, King Khalid University, Abha 62529, Saudi Arabia. [15]Department of Clinical Anatomy, Faculty of Medicine, King Abdulaziz University, Jeddah, Saudi Arabia. [16]Pre-Clinic Department, Faculty of Veterinary Science, Nangarhar University, Nangarhar 2603, Afghanistan. [17]Department of Forensic Medicine and Toxicology, Faculty of Veterinary Medicine, Benha University, Toukh 13736, Egypt. [18] Department of Biochemistry, Faculty of Veterinary Medicine, Qena University, Qena 83523, Egypt. ✉email: matta@kfu.edu.sa; afaridrawan@gmail.com; ahmed.abdeen@fvtm.bu.edu.eg

Environmental pollution caused by heavy metals poses a growing threat to public health and ecosystem integrity. Among these pollutants, the naturally occurring element chromium which can be found in soil, rocks, and volcanic dust[1]. It is primarily found in the form of potassium dichromate (Cr, $K_2Cr_2O_7$) and widely employed in industries including electroplating, leather tanning, and dye production[2]. In addition, Cr is difficult to eradicate from the environment and readily bioaccumulates throughout the food chain. Food and drinking water contaminated with Cr can expose the public to Cr, primarily in the vicinity of an area where Cr contamination has persisted for extended period of time[3]. It's high water solubility and strong oxidative properties make it a persistent and hazardous environmental pollutant[2,4]. Upon exposure, Cr can exert multi-organ toxicity, with the nephron being one of the principal target tissue due to its crucial role in filtration and detoxification[5]. The nephrotoxicity of Cr is well documented, primarily involving oxidative stress, mitochondrial dysfunction, inflammation, and apoptosis in kidney tissues[6]. However, its specific impact on renal water transport mechanisms, particularly the aquaporins (AQPs) family of water channels, remains poorly understood.

AQPs are integral membrane proteins channel that expedite the selective translocation of water through cell membranes, modulate osmolarity and playing a crucial role in renal concentration mechanisms[7,8]. The proximal convoluted tubule renders as the cardinal station of absorption for the fluids after being passed across the glomeruli, wherein AQP1 is notably upregulated[9,10]. AQP1 is essential for the renal tubule water permeability and countercurrent exchange mechanisms[11]. Conversely, AQP2 is particularly plentiful in the collecting ducts' epithelial cells, which play crucial function in maintaining the volume of fluid and concentration of urine[10]. According to certain reports, disruption of their expression or function can result in significant impairments in renal water handling and may contribute to acute renal damage and are helpful for diagnosing it early[12,13]. A growing body of research suggests that renal AQP1 and 2 may change in response to various insults, including puromycin[14], methotraxate[10], lipopolysaccharide[11], and gentamycine[7].

Consequently, the current study was done to investigate the nephrotoxic effects of Cr with a specific focus on alterations in renal AQP expression, providing insights into how environmental exposure to Cr may compromise renal water homeostasis. Kidney function parameters, levels of oxidative stress markers, and renal histology and electron microscopy were evaluated. And to investigate the possible mechanistic insights underline the toxic action of Cr on the renal tubular AQP1 and AQP2 proteins. Understanding these molecular disruptions could help clarify the pathophysiology of Cr-induced kidney injury and guide the development of protective or therapeutic strategies.

Materials and methods

Animals and experimental protocol

Thirty-six Wistar albino male rats weighing 190 ± 10 g was acquired from the Faculty of Veterinary Medicine, Benha University, Egypt. All of the animals were housed in an area with adequate ventilation, with a temperature and relative humidity of 25 ± 3 °C and ~ 50–60%, respectively. They also had free access to commercial pellets and water, were placed in a light/dark cycle that lasted for 12 h, and were given two weeks to adjust before the experiment began. Rats were randomized into three even groups (12 rats each); Control group, rats received distilled water only; Cr-Low group, rats received 2.5 mg/kg of Cr (Sigma-Aldrich, USA) intra-peritoneally; and Cr-High group, rats received 7.5 mg/kg of Cr intra-peritoneally. Cr was given every day for 14 days. This doses regimen was determined based on the previous reports[15,24,33]. At the end of the experiment, all rats were euthanized humanely by cervical dislocation.

Collection of blood and renal tissue

Upon completion of experiments, rats were anesthetized with 100% isoflurane. Blood was taken from the retro-orbital venous plexus. The serum was then extracted and kept for later biochemical analysis at − 20 °C. Then, all rats were euthanized and kidney tissues were dissected and cut into four parts, two parts for the histopathological and electron microscopy investigations; the other two parts were preserved at − 80 °C for gene expression and oxidative stress status analyses.

Hemato-biochemical study

An automatic blood cell counter was employed to evaluate the total WBCs count and hemoglobin. Moreover, sera were utilized for estimation of urea, and creatinine, lactate dehydrogenase (LDH), alkaline phosphatase (ALP) enzymatic activities, glucose, total bilirubin, total protein, albumin, and triglycerides (TG) concentrations using diagnostic kits acquired from Laboratory Biodiagnostics Company, Egypt. All analyses were performed according to the manufacturers' instructions.

Evaluation of oxidative stress markers

Renal malondialdehyde catalase (CAT), superoxide dismutase (SOD), malondialdehyde (MDA), reduced glutathione (GSH), and Glutathione peroxidase (GPx) were ascertained using commercial kits (Laboratory Biodiagnostics Company) and the procedure was performed in accordance with provider protocol.

mRNA expressions

The total RNA was isolated from tissue homogenates using the QIAamp RNeasy Mini Kit (Qiagen). RNA concentration and purity were determined with a NanoDrop ND-1000 spectrophotometer. Complementary DNA (cDNA) was synthesized from total RNA using the QuantiTect Reverse Transcription Kit (Qiagen, USA). Quantitative real-time PCR (qRT-PCR) was performed on a Rotor-Gene Q cycler with SYBR Green QuantiTect PCR kits to assess mRNA expression levels of kidney injury molecule-1 (KIM-1), AQP1, and AQP2. Primer sequences are provided in Table 1. Each 25 µL reaction mixture contained SYBR Green Master Mix, RevertAid Reverse Transcriptase, a specific primer (20 pmol), nuclease-free water, and RNA template. The thermal cycling protocol consisted of an initial activation at 95 °C for 15 min, followed by 40 cycles of denaturation at 94 °C for 15 s, annealing at 60 °C for 1 min, and extension at 72 °C for 30 s. Relative gene expression was calculated using the $2^{-\Delta\Delta Ct}$ method, with GAPDH serving as the endogenous control.

Histopathological analysis

The kidney tissue was preserved in 10% neutral buffered formalin for 24 h for histopathology. Subsequent to appropriate fixation, the kidney tissue was embedded in paraffin, cut into 5 µm thickness slices and stained with hematoxylin and eosin (H&E) for histopathological examination and periodic acid-Schiff (PAS) for evaluating basement membranes, brush boundaries, and tubule morphology. A light microscope integrated with digital imaging system (Nikon Eclipse E100, Japan) was used for histopathological evaluation and imaging.

Transmission electron microscopic examination (TEM)

For TEM evaluation, the renal cortical samples were cut into small pieces ($1mm^3$) and were fixed into buffered glutaraldehyde (2.5%) in phosphate buffer solution (pH 7.4) 0.1 M at 4 °C for 2 h. Specimens were processed for semi-thin (0.5 µm) and ultrathin (80 nm) sections. Grids were examined and photographed employing TEM JOEL (JEM-100 SX, Akishima, Tokyo, Japan).

Determination of chromium in renal tissue

Sample preparation (microwave digestion)

Approximately 250 mg of kidney tissue was subjected to acid digestion. Samples were digested using 9 mL of concentrated nitric acid (HNO_3, 69%, Merck, Germany) and 1 mL hydrogen peroxide (H_2O_2, 30%, Suprapur®, Merck) in a closed-vessel microwave digestion system (ETHOS UP, Milestone, Italy). The digestion program was set as follows: ramp to 200 °C over 15 min, hold at 200 °C for 20 min, and allow cooling to 50 °C before vessel opening. The digested samples were then quantitatively transferred and diluted to a final volume of 50 mL using Milli-Q water and filtered through a 0.45 µm PTFE syringe filter prior to analysis.

Inductively coupled plasma mass spectrometry (ICP-MS) analysis

Cr concentration was determined using an iCAP RQ ICP-MS system (Thermo Fisher Scientific, USA) equipped with a single quadrupole mass analyzer, nickel sampler and skimmer cones, and a Peltier-cooled spray chamber. Instrumental operating conditions were set as follows: RF power 1550 W; plasma gas flow 14 L/min Ar; auxiliary gas flow 0.8 L/min Ar; nebulizer gas flow 1.05 L/min Ar. Sample uptake and wash times were each set at 40 s using a peristaltic pump. Cr was quantified using the 52Cr isotope in kinetic energy discrimination (KED) mode to minimize potential polyatomic interferences. Data acquisition was performed in peak hopping mode with a dwell time of 10 ms per isotope and three replicate runs per sample.

Calibration and quality control

A calibration curve (0-100 ppb) was prepared using certified Cr standard solutions (LGC, Germany). Quality control samples were analyzed at 50 ppb to ensure analytical accuracy. The method was validated in terms of linearity, accuracy, and precision, showing excellent linearity for Cr ($R^2 > 0.999$), high recovery rates, and good repeatability with relative standard deviation (RSD < 5%), confirming the reliability of the analytical procedure.

Statistical analyses

First all data were tested whether they were normally distributed at $P > 0.05$ using Shapiro-Wilk's test. The homogeneity of variances among groups was also checked using Levene's test. Then all data were analyzed using one-way analysis of variance (ANOVA), and the treatment means were compared using Duncan's post hoc test using SPSS software, version 21; Inc., Chicago, USA. Significance was obtained at $P < 0.05$. The OriginPro software (version 2019b) was used to for univariate data visualization. The mean and 95% confidence interval are used to interpret each value. For multivariate analyses, "Factoextra" and "FactoMineR" packages were created in Rstudio using R version 4.0.2.

Gene	Forward (from 5' to 3')	Reverse (from 5' to 3')	Accession no.
KIM-1	TATTTGGGGGAACAG GTTGC	CAAGTCACTCTGGTTAGCCGTG	NM_001173393.2
AQP1	GGCTTCAATTACCCACTGGA	TTGATCCCACAGCCAGTGTA	NM_012778.2
AQP2	TGTCTC- CTTCCTTCGAGCTG	AGCTCTACAGTCACAGCCTG	NM_012909.3
GAPDH	GACATGCCGCCTGGAGAAAC	AGCCCAGGATGCCCTTTAGT	NM_017008

Table 1. List of primers used for real-time PCR analysis.

Results

Effects of Cr on hematological parameters

The values of Hb %, and WBCs following exposure to both concentrations of Cr are displayed in Fig. 1. The Hb % significantly declined at both Cr concentration confront to the control (Fig. 1A). Conversely, total number of WBCs significantly raised in following exposure to either dose of Cr (Fig. 1B). Nonetheless, Hb %, and WBCs upon Cr-High intoxication display significant changes confront to Cr-Low in a dose dependent way.

Biochemical parameters analyses

Cr induced nephrotoxicity as demonstrated by elevation of serum kidney biomarkers as depicted in Fig. 2. Both doses of Cr intoxication prompted a noticeable increase in kidney function tests (creatinine and urea levels) compared to control. Notwithstanding, rats with Cr-High exerted worthy significant injury than the lower dose as indicated by substantial increase in creatinine, and urea levels in response to high dose-Cr treatment in a dose-dependent pattern.

Additionally, a remarkable decrease in total protein and albumin levels were spotted following exposure to both Cr doses compared to control rats. On the contrary, protein and albumin levels in response to Cr-High were significantly decreased compared to Cr-Low that implied that high dose Cr-induced notable renal tissue damage in a dose dependent pattern (Fig. 2C and D, respectively). In contrast, the blood glucose level was dramatically enhanced upon exposure to both Cr doses compared to control. Nevertheless, nonsignificant difference was noticed between Cr-Low and Cr-High treatment (Fig. 2E).

The activities ALP and LDH were measured and displayed in Figs. 3A and B, respectively. A noticeable rise in ALP and LDH levels was spotted following exposure to both Cr dosages compared to control rats. Conversely, ALP and LDH levels upon Cr-High intoxication were considerably increased compared to Cr-Low implying that high dose Cr-induced significant renal tissue damage in a dose-dependent pattern.

Additionally, TG (Fig. 3D) and bilirubin (Fig. 3C) were assessed and exhibited markable increase following Cr intoxication. On the contrary, TG level upon Cr-High intoxication was considerably increased compared to Cr-Low, suggesting that high dose Cr-induced substantial renal tissue damage in a dose-dependent way. However, there was no discernible difference in bilirubin level between Cr-Low and Cr-High treatments.

Assessment of renal oxidative state

The effect of Cr intoxication on oxidative distress indices and lipid peroxidation (LPO) in kidney tissues is exhibited in Fig. 4. Remarkable increases in MDA level alongside worthy decreases in the concentration of GSH and activities of SOD, GPx, and CAT were noted in renal tissues upon exposure to both doses of Cr-intoxication in the contrary to the control rats. These findings confirmed the presence of oxidative damage following exposure to Cr. Intriguingly, on the other hand, Cr-High administration evoked significant induction of oxidative renal damage compared to Cr-low. These results revealed a dose-dependent Cr -prompted oxidative damage.

Assessment of renal AQP1, AQP2, and KIM-1 mRNA expressions

Renal expressions of AQP1, AQP2, and KIM-1 were investigated to demonstrate the nephrotoxic consequences of Cr exposure (Fig. 5). Both AQPs demonstrated a substantial downregulation following exposure to Cr (high

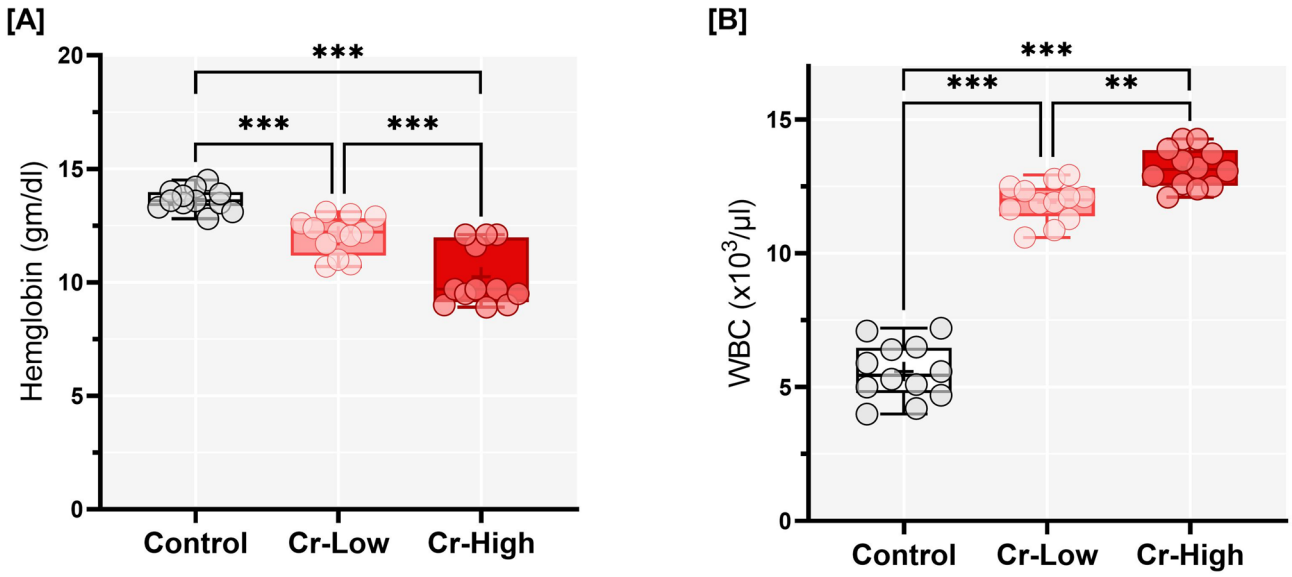

Fig. 1. Effects of potassium dichromate (Cr) on hematological parameters. Dot-box plots exhibit (**A**) hemoglobin (Hb) concentration and (**B**) total white blood cell (WBC) count in the Control group and groups treated with a low dose (2.5 mg/kg bw) or high dose (7.5 mg/kg bw) of Cr for 14 days. Significance was determined by one-way ANOVA followed by Duncan's post hoc test (**$P < 0.01$; ***$P < 0.001$). The mean and 95% confidence interval are presented for each group.

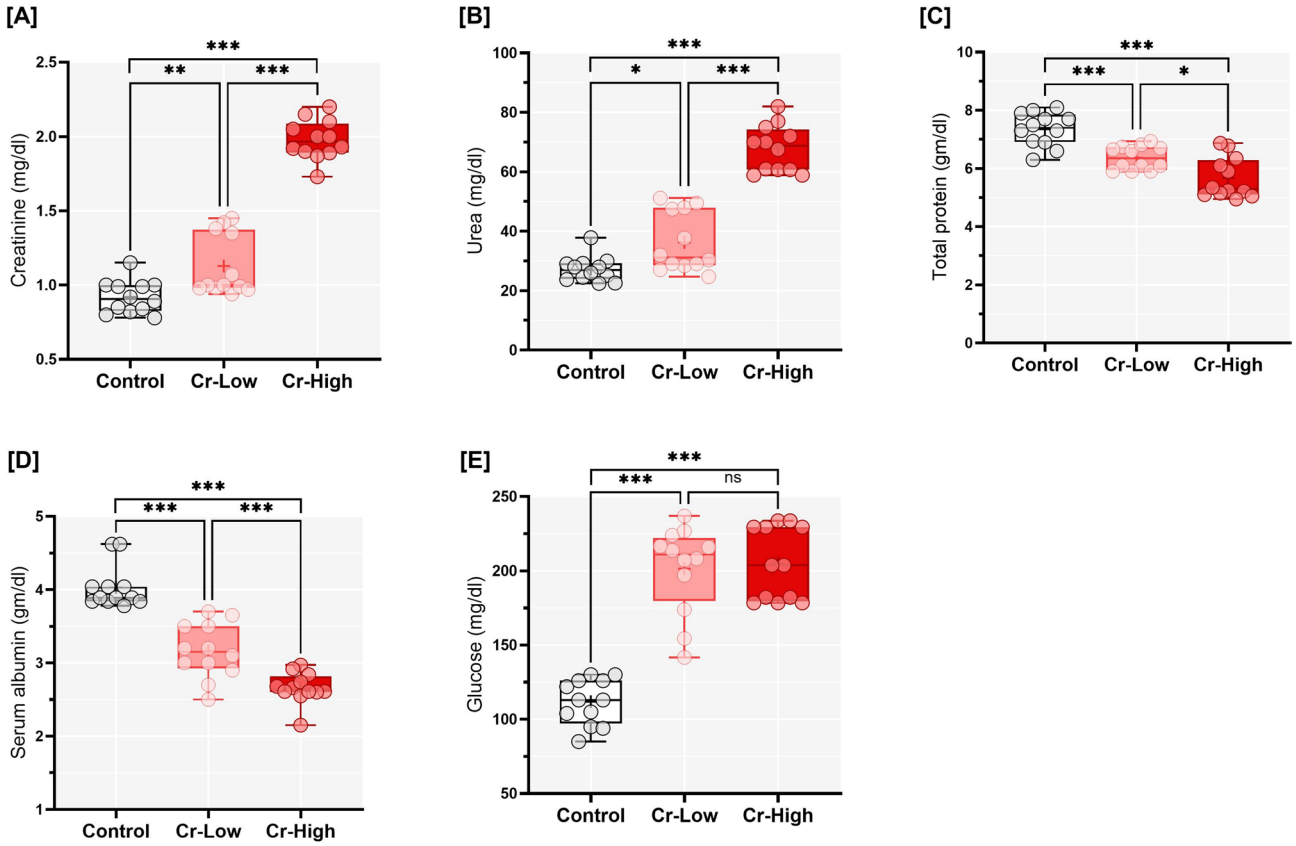

Fig. 2. Effects of potassium dichromate (Cr) on renal function and blood parameters. Dot-box plots present (**A**) serum creatinine, (**B**) serum urea, (**C**) total protein, (**D**) serum albumin, and (**E**) blood glucose levels in the Control group and groups treated with a low dose (2.5 mg/kg bw) or high dose (7.5 mg/kg bw) of Cr for 14 days. Significance was determined by one-way ANOVA followed by Duncan's post hoc test (*$P < 0.05$; **$P < 0.01$; ***$P < 0.001$; ns, non-significant). The mean and 95% confidence interval are presented for each group.

and low dosage) compared to controls (Figs. 5A and B, respectively). On the other hand, Cr-High significantly reduced detection of gene expression of AQP1 and AQP2 in kidney tissue compared to Cr-Low. Moreover, higher expression of KIM-1 in renal tissue on exposure to low and high dosage of Cr was noticed (Fig. 5C). While exposure to high Cr dose, we noticed a considerable increased gene expression of KIM-1 in renal tissue compared to low Cr dosage.

Histoarchitecture findings

Renal sections of the Control group displayed normal histological features, such as normal renal tubules, glomeruli, and blood vessels (Fig. 6A). Meanwhile, the histoarchitectural examination of kidney tissue from rats intoxicated with a low dose of Cr revealed mild to moderate glomerular degeneration with focal periglomerular lymphocytic infiltration (Fig. 6B). Congestion of renal blood vessels and glomerular tufts with slight vacuolation in their tunica intima. All renal tubules in the renal cortex displayed vacuolation, degeneration and desquamation of their lining epithelium with the formation of epithelial or hyaline casts in their lumen (Figs. 6B and C). The most characteristic lesion is renal necrosis of cortical tubular epithelium which manifested as highly eosinophilic cytoplasm with pyknotic nuclei (Fig. 6C).

Interestingly, these alterations were significantly exhibited in the renal section from rats given a high dose of Cr as glomerular tuft shrinkage, necrosis, increased Bowman's space with cystic dilation of some renal tubules was also observed (Fig. 6D). Most of the renal tubules exhibited severe necrosis in the form of diffuse coagulative necrosis (Fig. 6E). Renal blood vessels showed marked endothelial cell proliferation and vesiculation in their wall, as well as perivascular oedema. Additionally, extensive recruitment of inflammatory cells in renal interstitial tissue, especially in the periglomerular and perivascular area (Fig. 6F).

PAS staining of renal tissue of the control group proved typical glomerular and renal tubules pattern no proteinaceous material buildup (Fig. 6G). The kidney sections from rats intoxicated with a low dose of Cr stained with PAS revealed mild fragmentation of the brush border of cortical renal tubules and proteinaceous cast in their lumen which showed positive PAS reaction (Fig. 6H). However, the PAS-stained kidney tissues from a Cr-High group showed either entire loss or noticeable disintegration of the proximal convoluted tubules' brush border (Fig. 6I).

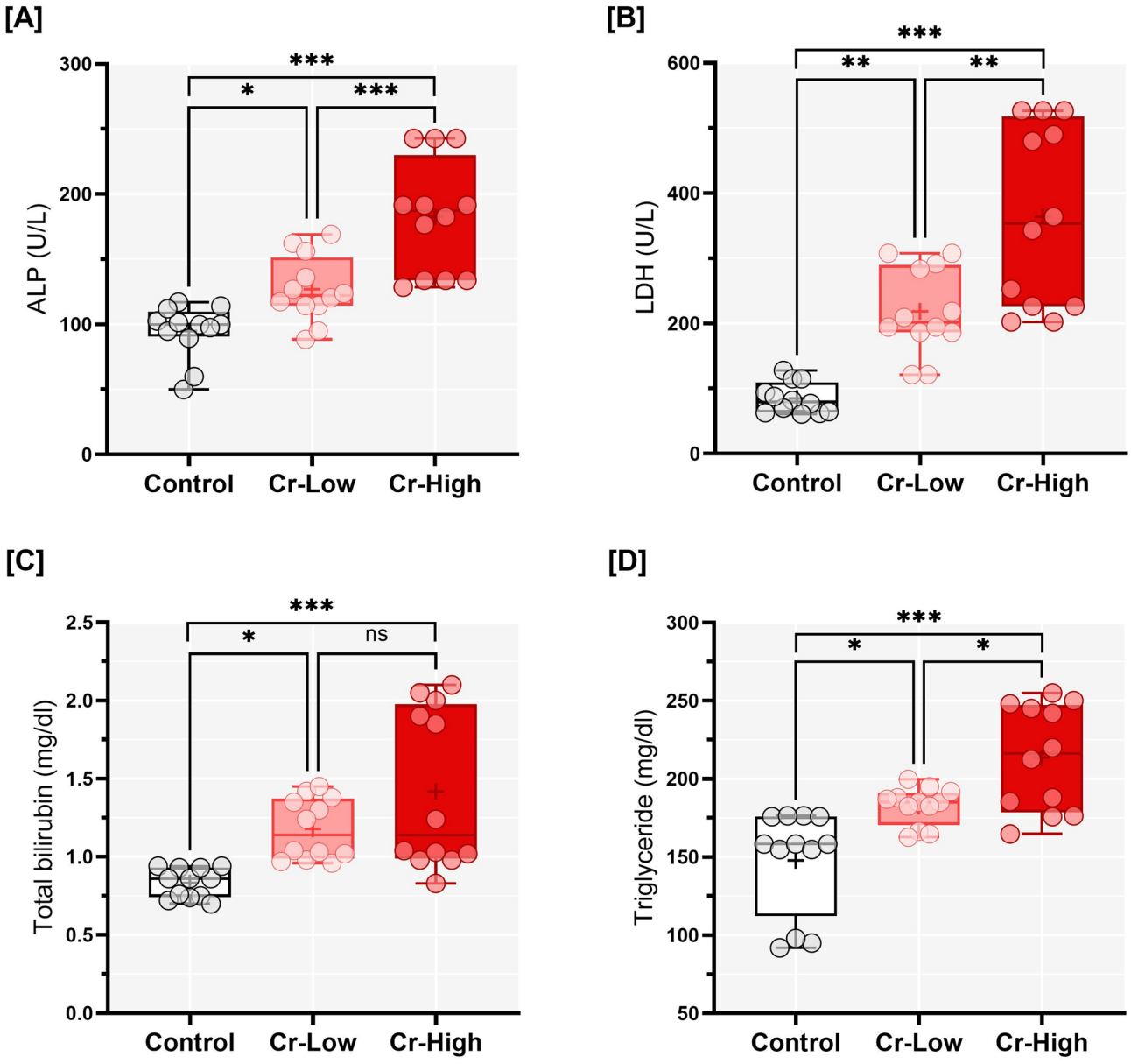

Fig. 3. Effects of potassium dichromate (Cr) on renal biochemical parameters. Dot-box plots showing (**A**) alkaline phosphatase (ALP) activity, (**B**) lactate dehydrogenase (LDH) activity, (**C**) total bilirubin, and (**D**) triglyceride (TG) levels in the Control group and groups treated with a low dose (2.5 mg/kg bw) or high dose (7.5 mg/kg bw) of Cr for 14 days. Significance was determined by one-way ANOVA followed by Duncan's post hoc test (*$P<0.05$; **$P<0.01$; ***$P<0.001$). The mean and 95% confidence interval are presented for each group.

Electron microscopic evaluation

As depicted in Fig. 7, In control group, the electroscopic examination of renal tissue displayed large cell cuboidal cell resting on thin regular basement membrane lining of proximal convoluted tubules. The cell reveals rounded basal nucleus, apical profuse long crowded microvilli, and multiple elongated mitochondria situated in the basal invaginating folds along the basal membrane. The distal convoluted lined with cuboidal cells resting on basement membrane, with smaller rounded nucleus and short few apical microvilli, and fewer mitochondria in the basal part. Collecting duct lined by low cuboidal pale staining principal cell with rounded nucleus. Endothelial cells with oval nucleus lining the lumen of glomerular capillary. The cytoplasm gives primary and secondary processes. The glomerular filtration barrier appears as tri-laminar structure showing regularity.

In Cr intoxicated groups, the cell of the proximal convoluted lining epithelium resting on irregular basement membrane with collagen deposition in the underlying connective tissue. The cytoplasm shows denser nucleus and multiple vacuoles. Moreover, the cell of distal convoluted tubules resting on deformed basement membrane and appears with rarified cytoplasm filled with small mitochondria. TEM further revealed small apoptotic mesangial cells with dense nuclei and heterogeneous mesangial matrix deposition, along with effacement of

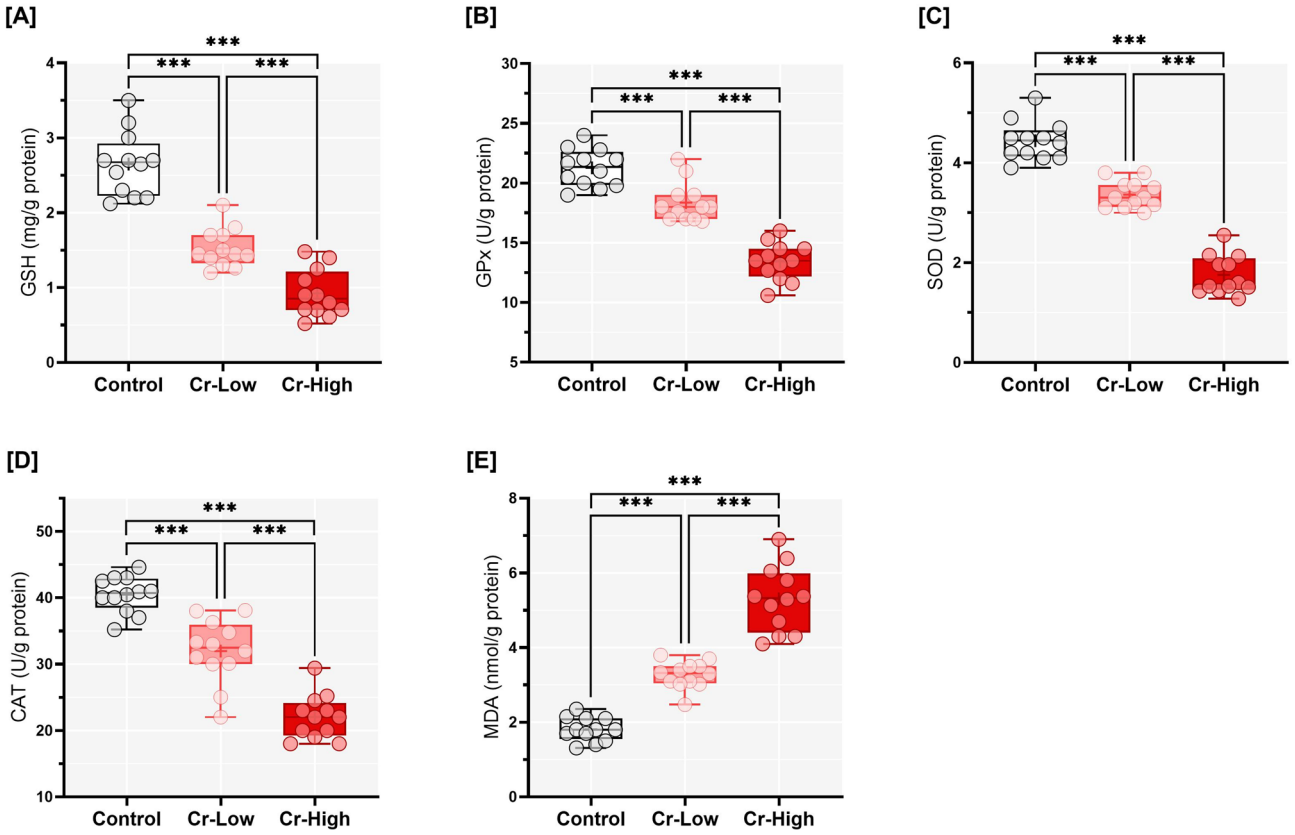

Fig. 4. Effects of potassium dichromate (Cr) on renal oxidative stress markers. Dot-box plots showing (**A**) reduced glutathione (GSH) level, (**B**) glutathione peroxidase (GPx) activity, (**C**) superoxide dismutase (SOD) activity, (**D**) catalase (CAT) activity, and (**E**) malondialdehyde (MDA) level in kidney tissues of the Control group and groups treated with a low dose (2.5 mg/kg bw) or high dose (7.5 mg/kg bw) of Cr for 14 days. Significance was determined by one-way ANOVA followed by Duncan's post hoc test (***$P < 0.001$). The mean and 95% confidence interval are presented for each group.

podocyte secondary processes. Large areas of early collagen fiber bundles and debris filling the spaces were noticed. The glomerular membrane appears irregular with areas of focal thickening. Likewise, podocyte exhibited effacement of secondary processes obliterating the filtration slits (Fig. 7). These ultrastructural changes provide direct evidence of mesangial cell apoptosis, which likely contributes to glomerular dysfunction and the observed alterations in filtration barrier integrity following Cr exposure.

Chromium bioaccumulation in renal tissues

In order to determine the concentration of Cr in renal tissues, potassium dichromate was used to evaluate the rate of bioaccumulation of Cr in these tissues. The results of this study show that renal Cr levels were significantly higher in both Cr-treated groups compared to the control group, as illustrated in Fig. 8. Interestingly, Cr accumulation exhibited a clear dose-dependent pattern, with Cr-High showing a significantly higher concentration than Cr-Low. These findings confirm that Cr is readily accumulated in kidney tissues following systemic exposure.

Multivariate analyses

To figure out the correlation between all measured covariates and treated groups, multivariate analyses were implemented as depicted in Fig. 9. The principal component analysis (PCA) plots demonstrated a clear separation among the three groups (Control, Cr-Low, and Cr-High). Biplot PCA model demonstrates two PC; PC1 (63.5%) accounts for the majority of the variance and PC2 (8.8%) further contributes to the discrimination but to a smaller extent. The Control group was strongly associated with elevated antioxidant and renal-protective markers, including GSH, SOD, CAT, and total proteins, as well as the expression of AQP1 and AQP2 mRNA. These variables point toward preserved renal function and oxidative balance. In contrast, the Cr-High-induced group are positively associated with classical markers of oxidative stress and renal injury, such as MDA, LDH, WBC count, and KIM-1 mRNA along with the renal Cr concentration. The strong loading vectors for these parameters indicate their major contribution to Cr-induced nephrotoxicity. The Cr-Low group occupies an intermediate position, reflecting a milder degree of disturbance. Furthermore, the 3D PCA plot (PC1, PC2, and PC3) distinguished all variables, which together accounted for 77.6% of the variation. PC1 represented for the majority of the variables studied and expressed the greatest percentage of variation (63.5%) whilst PC2 and PC3 showed smaller proportions of percentage (8.8% and 5.3%, respectively). The PCA demonstrated that the Cr-

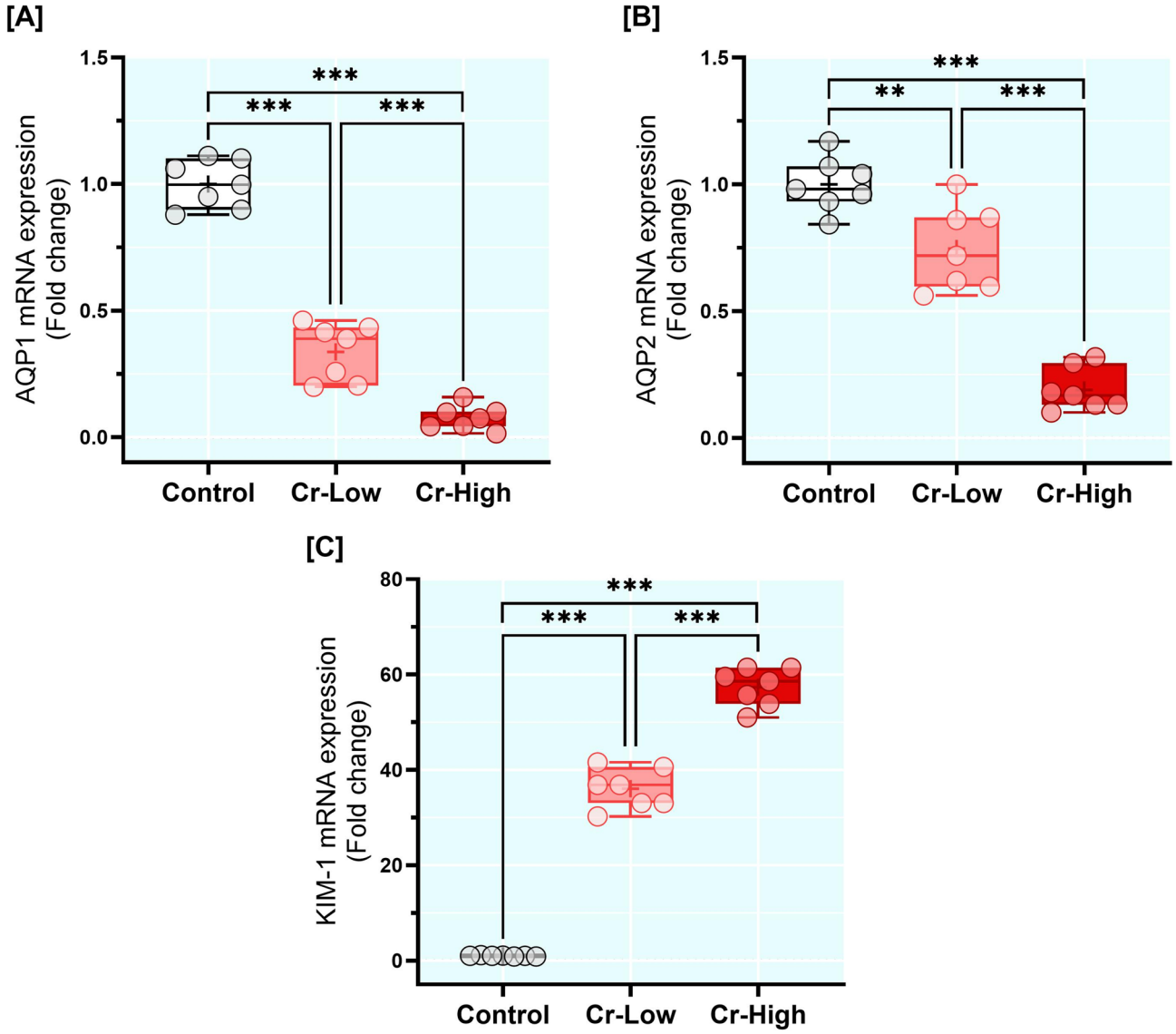

Fig. 5. Effects of potassium dichromate (Cr) on renal mRNA expression of aquaporins and kidney injury molecule-1. Dot-box plots show the mRNA expression levels of (**A**) aquaporin-1 (AQP1), (**B**) aquaporin-2 (AQP2), and (**C**) kidney injury molecule-1 (KIM-1) in renal tissues of the Control group and groups treated with a low dose (2.5 mg/kg bw) or high dose (7.5 mg/kg bw) of Cr for 14 days. Relative gene expression was calculated using the $2^{-\Delta\Delta Ct}$ method with GAPDH as the endogenous control. Significance was determined by one-way ANOVA followed by Duncan's post hoc test (**$P<0.01$; ***$P<0.001$). The mean and 95% confidence interval are presented for each group.

High group was clearly distinct from the Control and Cr-Low groups, which clustered on the left side with each other and secluded from the Cr-High-exposed one (Fig. 9A).

Moreover, the variable importance in projection (VIP) scores is exhibited in Fig. 9B and demonstrated that glucose, creatinine, WBC count, urea, GSH, oxidative markers, KIM-1 and AQPs mRNA expressions, and Cr residue were the most influential variables in the current study. VIP score indicating that alterations in inflammatory response, oxidative balance, and protein metabolism are key drivers distinguishing the Cr-High group from the other groups. Furthermore, low AQPs mRNA expressions emphasize the contribution of impaired water transport in Cr-High intoxication. Additionally, the correlation analysis highlights biomarkers most strongly associated with creatinine elevation in the damaged rats. A pattern hunter plot correlation coefficient exhibited strong positive correlation between serum creatinine level and Cr residue, KIM-1, bilirubin, glucose, ALP, TG, WBCs, LDH, urea, and MDA. Moreover, there was negative correlation between serum creatinine and AQP1, AQP2, total protein, GSH, Hb, albumin, GPx, CAT, and SOD levels, this reflects a decline in antioxidant capacity and protein homeostasis in the presence of renal impairment (Fig. 9C).

Over and above, the clustering heatmap provides a clear visual interpretation of every dataset (Fig. 9D) and displays a considerable discrepancy in the concentration of all evaluated parameters in respect to Cr-High

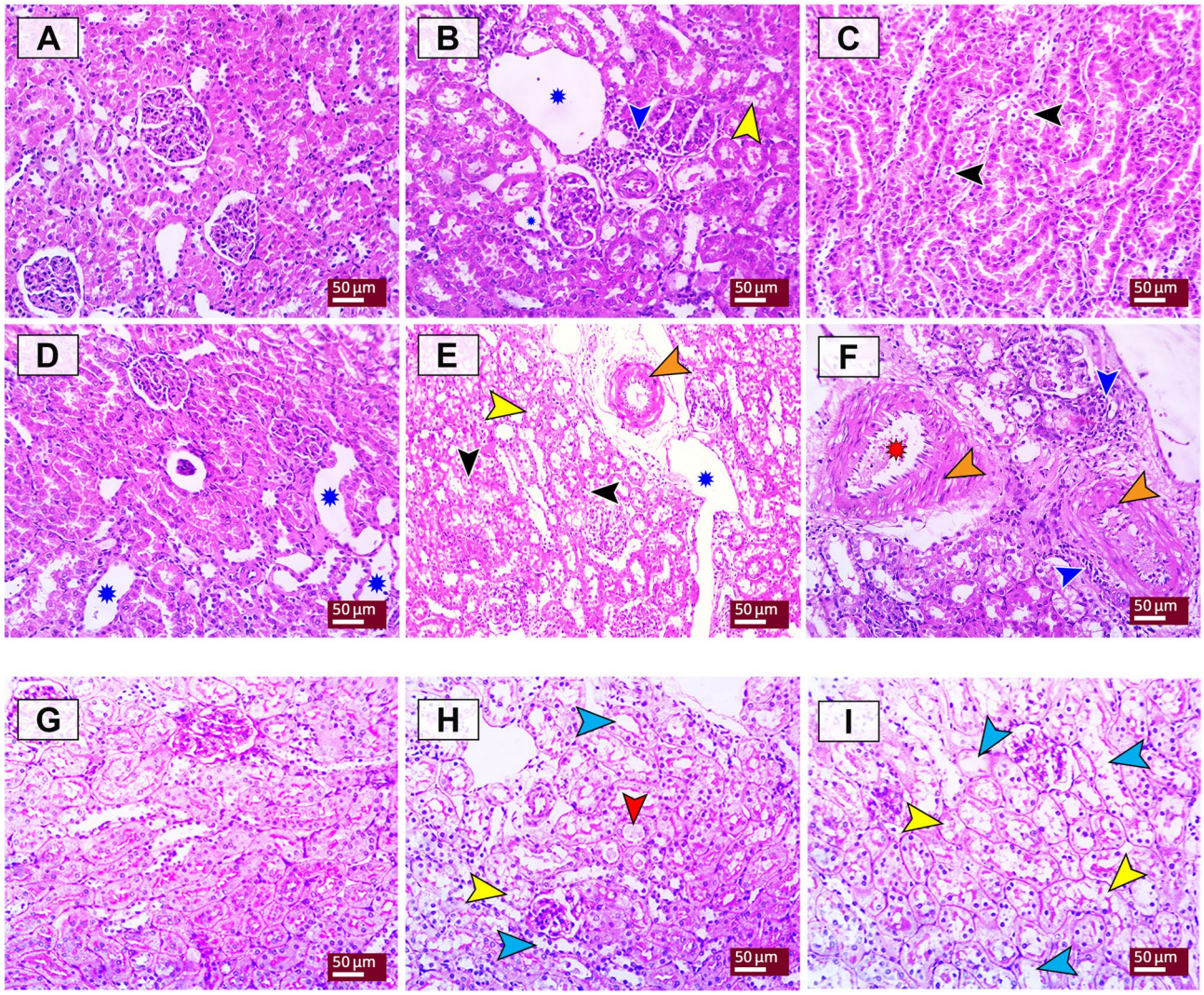

Fig. 6. Histopathological alterations in renal tissue of rats following potassium dichromate (Cr) exposure. Photomicrographs of kidney sections stained with hematoxylin and eosin (H&E; **A**-**F**) and periodic acid-Schiff (PAS; **G**-**I**) from control and Cr-treated rats. (**A**-**F**) H&E-stained sections: (**A**) Control group showing normal architecture of renal glomeruli and tubules. (**B**-**C**) Cr-Low group (2.5 mg/kg): (**B**) Periglomerular and perivascular lymphocytic infiltrations, tubular epithelial hydropic degeneration, and tubular dilatation. (**C**) Renal tubular lining epithelium with pyknotic nuclei. (**D**-**F**) Cr-High group (7.5 mg/kg): (**D**) Tubular cystic dilation. (**E**) Extensive tubular epithelial hydropic degeneration, tubular dilatation, and pyknotic nuclei. (**F**) Congestion of renal blood vessels with marked endothelial proliferation, vacuolation of the vessel wall, and severe perivascular edema admixed with mononuclear leukocytic infiltration. (**G**-**I**) PAS-stained sections: (**G**) Control group revealing normal cytoarchitecture of renal corpuscle with intact Bowman's capsule and brush border of proximal convoluted tubules showing positive PAS reaction. (**H**) Cr-Low group showing mild loss of brush border in the proximal convoluted tubules with PAS-positive hyaline cast. (I) Cr-High group showing severe loss of brush border of in the proximal convoluted tubules.

toxicity compared to other groups. Cr-High group forming a distinct cluster characterized by elevated levels of renal Cr concentration, MDA, ALP, urea, creatinine, TG, LDH, and KIM-1 mRNA along with lower expressions in the APQs mRNA levels. These findings posit that the Cr-High group revealed greater injury than the other groups.

Ultimately, as exhibited on Fig. 10, a volcano plot was used to easily visualize the most significant differences between groups. It represent a scatter plot of the negative $\log^{10}$-transformed P-values obtained from a particular t-test in relation to the log2-fold change in expression. According to our data, WBCs, MDA, glucose, LDH, bilirubin, KIM-1, TG, ALP, urea, creatinine, and Cr residue were remarkably increased in Cr-Low exposed rats compared to the controls, indicating an early oxidative and inflammatory response (Fig. 10A). Notably, KIM-1 mRNA exhibited a strong positive log2(FC) and high significance, marking it as the most sensitive early kidney injury biomarker under low-dose Cr stress. In contrast, AQP1 and AQP2 mRNA showed slight downregulation, suggesting early disruption in renal water-handling pathways.

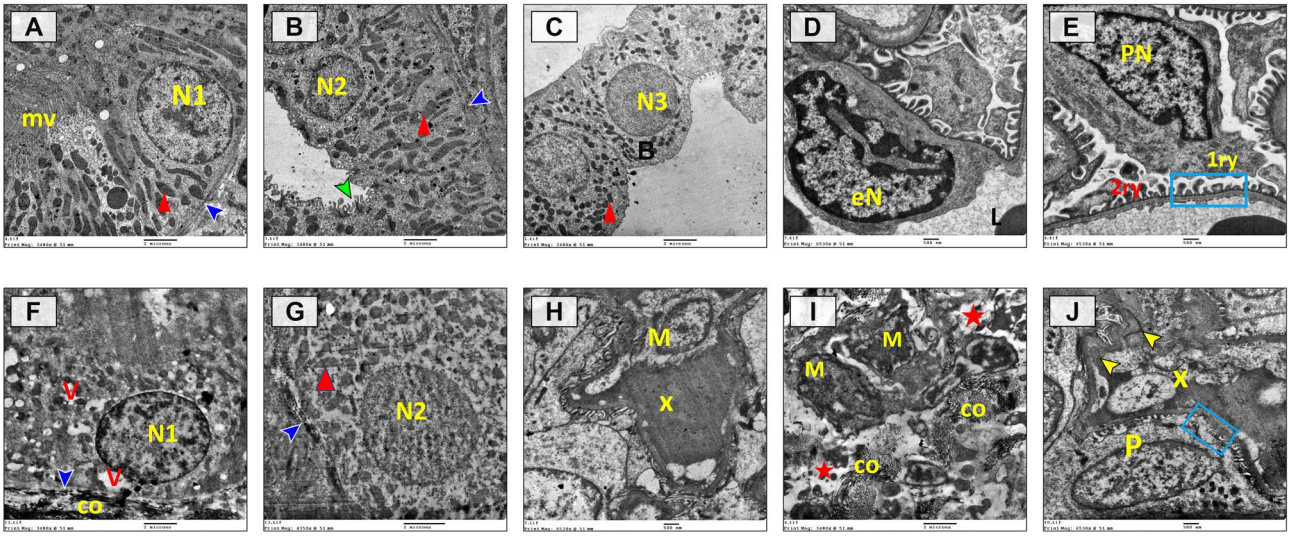

Fig. 7. Transmission electron microscopy (TEM) micrographs of renal tissue from control and potassium dichromate (Cr)-treated rats. Representative ultrastructural images of kidney sections from control rats (**A**-**E**) and rats treated with Cr (F-J). (A-E) Control group: (**A**) Proximal convoluted tubule (PCT) lining epithelium showing a large cuboidal cell resting on a thin regular basement membrane (blue arrow). The cell reveals a rounded basal nucleus (N1), apical profuse long crowded microvilli (mv), and multiple elongated mitochondria (red arrow) situated in basal invaginating folds along the basement membrane. (**B**) Distal convoluted tubule (DCT) lining epithelium showing cuboidal cells resting on basement membrane (blue arrow), with a smaller rounded nucleus (N2), short few apical microvilli (green arrow), and fewer mitochondria (red arrow) in the basal part. (**C**) Collecting duct epithelium exhibiting a low cuboidal pale-staining principal cell with a rounded nucleus (N3) and mitochondria (red arrow). (**D**) Endothelial cell with oval nucleus (eN) lining the lumen of a glomerular capillary (L). (**E**) Large podocyte with its nucleus (PN). The cytoplasm gives primary (1ry) and secondary (2ry) processes. The glomerular filtration barrier appears as a regular tri-laminar structure (rectangle). (**F**-**J**) Cr-treated groups: (**F**) PCT lining epithelium resting on an irregular basement membrane (blue arrow) with early collagen fiber bundles deposition in the underlying connective tissue (co). The cytoplasm shows a denser nucleus (N1) and multiple vacuoles (v). (**G**) DCT lining epithelium appearing with rarified cytoplasm filled with small mitochondria (red arrow). A deformed basement membrane is apparent (blue arrow). (H) Small apoptotic mesangial cell (M) with deposition of a large amount of mesangial matrix (x). (I) Multiple apoptotic mesangial cells with dense nuclei (M), large areas of early collagen fiber bundles (co), and debris filling the spaces (star). (**J**) Irregular glomerular membrane with areas of focal thickening (yellow arrows). Podocyte (P) showing effacement of secondary processes obliterating the filtration slits (rectangle). The mesangial matrix appears heterogeneous (x).Al-ShahedAl-Shahed

Moreover, high-dose Cr exposure caused marked biochemical and molecular disturbances, as reflected by the strong shift in most variables and high statistical significance. Creatinine, WBCs, urea, MDA, glucose, LDH, ALP, TG, bilirubin, KIM-1, and Cr residue were pronounced increase in Cr-High group confrontation with control rats (Fig. 10B). These markers showed strong positive log2(FC) values, highlighting substantial renal impairment and systemic metabolic disruption. On the contrary, antioxidant markers (SOD, CAT, GPx, GSH) exhibited significant reduction. This downward shift reflects severe oxidative depletion and failure of endogenous defense mechanisms. Molecularly, KIM-1 mRNA again showed the most dramatic upregulation, confirming severe tubular injury under high-dose of the Cr exposure. Meanwhile, AQP1 and AQP2 mRNA were significantly reduced, indicating major impairment in tubular transport and water reabsorption processes.

Furthermore, when Cr-High group compared versus Cr-Low group as depicted in Fig. 10C, several injury markers (creatinine, urea, MDA, WBCs, ALP, LDH, TG) were significantly increased confirming progressive deterioration of renal and oxidative parameters with increasing Cr exposure that highlights the dose-dependent nature of Cr-induced toxicity. Antioxidant enzymes (SOD, GPx, CAT, GSH) were dramatically more suppressed in Cr-High, reflecting a sharper oxidative imbalance. As seen previously, expression of AQP1 and AQP2 mRNA remained markedly reduced, suggesting that tubular functional damage worsens with dose escalation. Notably, KIM-1 mRNA did not increase further compared to the already-high elevation at low dose, suggesting that KIM-1 may plateau at high injury levels, while biochemical markers (creatinine, urea, MDA) continue to escalate. This comparison confirms that high-dose Cr exacerbates renal oxidative stress, inflammation, and functional impairment far beyond the changes seen in the lower dosage.

Discussion

It is well recognized that exposure to Cr in the environment and in the workplace may be nephrotoxic to both humans and animals. Cr is mainly eliminated by the kidneys, where it builds up and damages the kidneys[15]. The detrimental effects of Cr are triggered by an excess of reactive oxygen species (ROS) generated during its

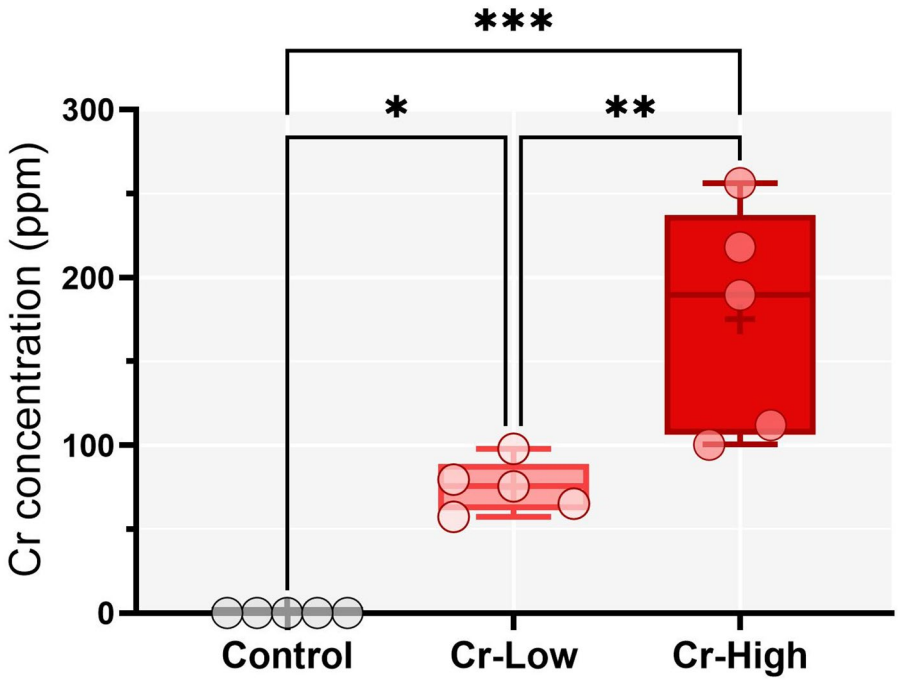

Fig. 8. Renal chromium bioaccumulation following potassium dichromate (Cr) exposure. Dot-box plot show chromium (Cr) concentration (ppm) in kidney tissues of the Control group and groups treated with a low dose (2.5 mg/kg bw) or high dose (7.5 mg/kg bw) of Cr for 14 days. Significance was determined by one-way ANOVA followed by Duncan's post hoc test (*P < 0.05, **P < 0.01, ***P < 0.001). The mean and 95% confidence interval are presented for each group.

metabolism, which promotes oxidative stress, necrotic cell death, and apoptosis[16]. Consequently, our findings expound noteworthy oxidative renal tissue disruption upon Cr treatment, as evidenced by a significant decrease in GPx, SOD, CAT activities and GSH level in renal tissues in a dose dependent manner. Remarkably, SOD is an intrinsic enzyme that acts as the first line of enzymatic defense. It quickly catalyzes $O_2^{\bullet-}$ dismutation to O_2 and H_2O_2, which is eventually gets quenched by GSH[17–21]. Astonishingly, CAT, on the contrary, breaks down the generated H_2O_2 to molecular oxygen and water, thereby helping in halting the induced oxidative damage[22,23]. GPx catalysis the conversion of peroxide into a non-toxic hydroxyl molecule, thus preserving redox equilibrium and inhibiting LPO, which helps protect the integrity of the cell membrane[16]. Notwithstanding, when these enzymes were exhausted, as displayed in our Cr-intoxicated group, $OH^{\bullet}$ radicals were produced in enormous amounts via Fenton's reaction. $OH^{\bullet}$ is the main deleterious reactive radical, which actively degrading the membrane lipids promoting LPO and MDA production in the tissues[24–26]. To make matters worse, MDA itself can bind to DNA and proteins, resulting in formation of adducts causing biomolecular damage, further complicating matters[7,24,27].

Accordingly, the current study confirmed the presence of membrane damage by demonstrating worthy increases in MDA levels in renal tissues. Consistent with these results obtained by previous reports[2,28,29], where, they validated increased MDA production following exposure to Cr. Our oxidative/antioxidant results in line with those of previous research that revealed cellular antioxidant incompetence in the renal tissue upon Cr exposure[5,16,30,31]. As anticipated, the integrity of the renal cells' membrane was compromised by elevated levels of LPO. This detrimental impact of oxidative stress on renal tubular membrane was corroborated by the current investigation following Cr intoxication. Fundamentally, mitochondria are the primary target of oxidative injury. Consequently, the proximal tubules' higher mitochondrial density enhanced their vulnerability to ROS-prompted oxidative hurt and apoptotic damage[32]. This is indicated by the corruption of the brush border of cortical tubules, irregular basement membrane with appearance of early collagen fiber bundles as shown in our histological and TEM morphology assessment, respectively. Additionally, the PAS findings confirmed that Cr has a substantial detrimental effect on renal tissues. Consistent with a prior study, microscopic analysis of kidney tissue treated with Cr revealed evidence of Cr-induced nephrotoxicity in the form of vacuolation, glomerular tufts, and congested glomerular capillaries in the tubular epithelial[5,16,28,33].

Consequently, a tubular dysfunction in our investigation occurred following Cr exposure, evidenced by a substantial elevation of serum levels of renal biomarkers (urea, creatinine) in a dose-dependent pattern thus uncovering the existence of severe deterioration in kidney function. The enhanced level of creatinine and urea could be due to the malfunction of glomerulus, which are the structures control the renal filtration. The increase in urea could also be explained by the enhanced proteins catabolism[34]. On the other side, current study also revealed increase LDH, and ALP following Cr intoxication. LDH, and ALP are the most sensitive biomarkers directly incriminated in the degree of cellular injury and toxicity because they are confined in the cytosol and are freed into the circulation after cellular hurt as a result of loss of membrane integrity; thus, they are deemed

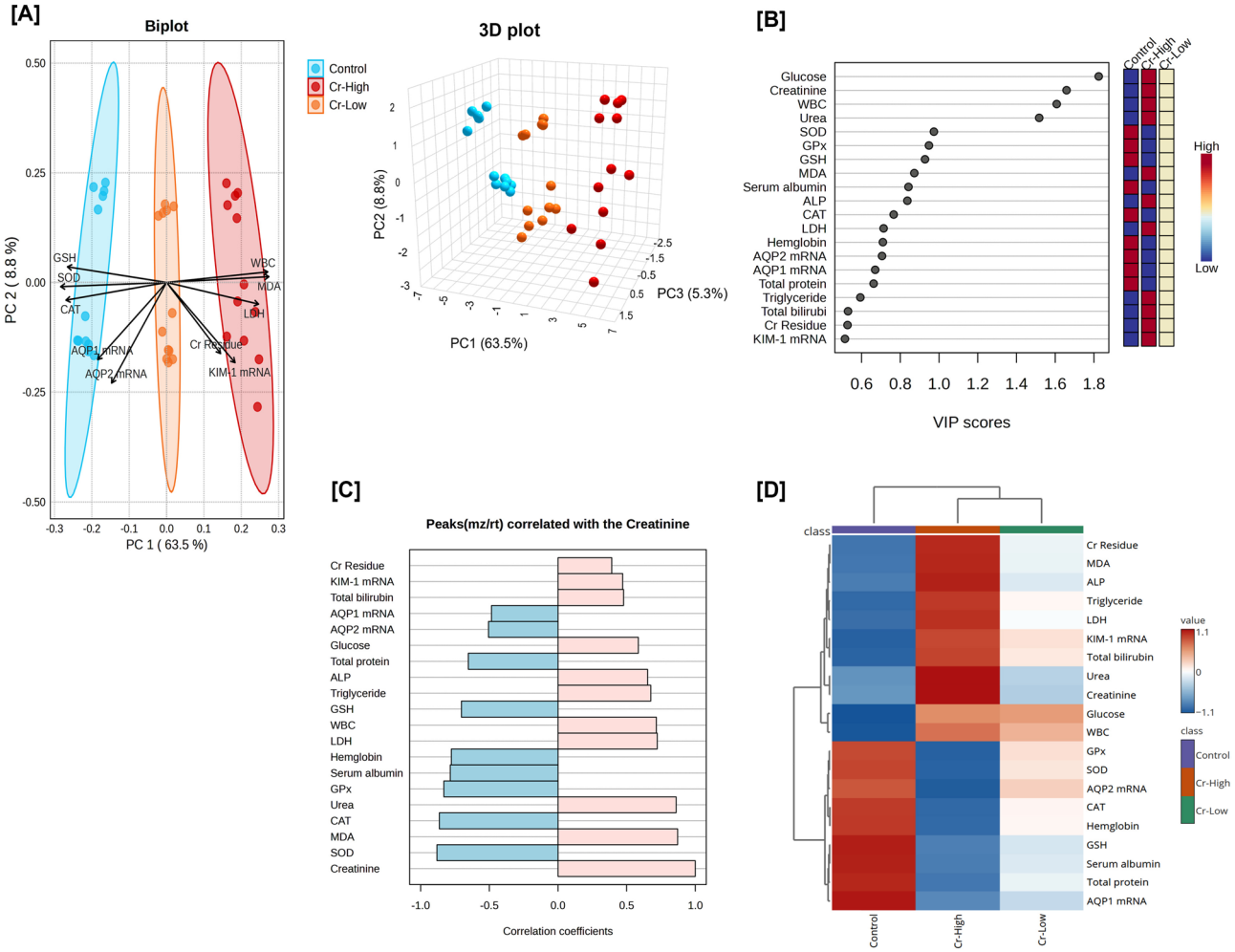

Fig. 9. Multivariate analyses of all data sets following potassium dichromate (Cr) exposure. Comprehensive statistical analysis integrating biochemical, molecular, hematological, and Cr residual parameters from control and Cr-treated rats (low dose: 2.5 mg/kg; high dose: 7.5 mg/kg). (**A**) Principal component analysis (PCA): Biplot score (PC1 vs. PC2, left) and 3D PCA plot (PC1, PC2, and PC3, right) showing the distribution of all variables and experimental groups. PC1 accounts for 63.5% of the variance, while PC2 and PC3 account for 8.8% and 5.3%, respectively. The Control group separated from the Cr-High group; while, the Cr-Low groups clustered in the middle, indicating dose-dependent toxic effects. (**B**) Variable importance in projection (VIP) scores: The gradation scaling from blue (lowest) to red (highest) indicates the contribution strength of each variable to group discrimination. (**C**) Pattern hunter plot correlation coefficient: Bars show the correlation of various parameters with serum creatinine levels. Pink bars indicate positive correlation (Pearson $r > +0.5$), while blue bars indicate negative correlation (Pearson $r < -0.5$). (**D**) Clustering heatmap: Each colored cell represents the concentration value of a parameter, with rows representing different parameters and columns representing treatment groups.

markers of renal damage[34,35]. Taking together, current data reveal that Cr obviously promotes renal dysfunction, as evidenced by deterioration of renal function as well as dramatic histological and electron microscopic degenerative changes of the kidney tissues in a dose-dependent way. These findings were in concordance with beforehand investigations[28,29,36]. In the same vein, Salama et al.[37] and Barhoma[15] also reported a significant renal injury with increased renal function following Cr exposure. This could be explained by renal tubule deformation and kidney loss of functional integrity brought on by Cr administration[29].

Blood acts as a pathological reflector of toxicants in subjected animals[34]. Consistent with this assertion, our study indicates changes in WBCs count and Hb concentration upon Cr exposure in a dose dependent pattern. WBCs act as guardians from pathogens and typically increase in case of infection. Therefore, the rise in WBCs in our investigation can be explained by the fact that Cr was identified as a toxicant and induce inflammatory response. Hb concentration is related to the total population of RBCs in blood. The reduction in Hb concentration implies that Cr could disrupt the erythropoietin release, which is the humoral regulator of red blood cell formation or intracellular conversion of Cr (VI) to Cr (III), which ultimately bind to Hb[38,39]. The present results are in the same vein with the findings of Adjroud et al.[40] in rats, Momo et al.[34] in rabbit and Islam et al.[41] in catfish treated with Cr. In addition, the changes in TG level after Cr exposure in the current study may

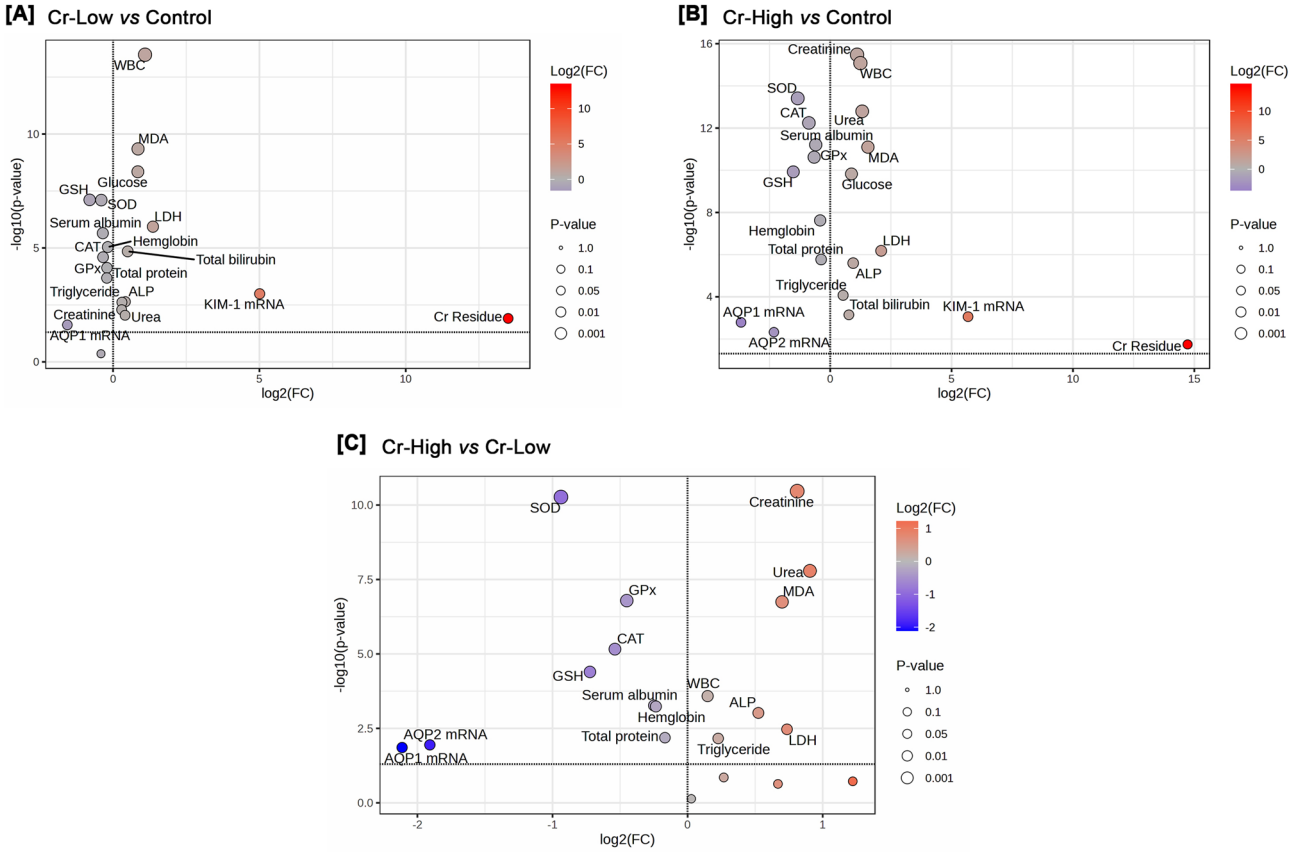

Fig. 10. Volcano plots of differential biochemical and molecular responses to potassium dichromate (Cr) exposure. (**A**) Cr-Low vs. Control: Cr residue and KIM-1 mRNA show the strongest positive log2FC and highest significance, marking it as the most sensitive early kidney injury biomarker. AQP1 and AQP2 mRNA show slight downregulation, suggesting early disruption of renal water-handling pathways. (**B**) Cr-High vs. Control: Cr residue and KIM-1 mRNA show the most dramatic upregulation, confirming severe tubular injury, while AQP1 and AQP2 mRNA are significantly reduced, indicating major impairment in tubular transport and water reabsorption. (**C**) Cr-High vs. Cr-Low: Direct comparison between high and low doses demonstrates progressive dose-dependent toxicity. Injury markers are significantly increased in the high-dose group. AQP1 and AQP2 mRNA expression remains markedly reduced, indicating worsening tubular functional damage with dose escalation. Notably, KIM-1 mRNA does not increase further compared to the already-high elevation at low dose, suggesting possible plateauing at high injury levels while biochemical markers continue to escalate.

indicates disruption of activities of lipase enzyme, leading to increase in plasma TG level[34,38]. The greater the tissues possess Cr, the increased inclination for Cr-induced oxidative distress to take place, which alters several metabolic pathways and persuades toxicity[38].

Interestingly, we noticed that Cr intoxication had been accompanied with downregulation of AQPs expression in kidney tissue. AQPs are transmembrane proteins channel that facilitate fluid transfer, modulate urine's osmolarity and concentration, and volume of fluids[8,42]. AQP1 is essential for tubule water permeability and countercurrent exchange activates[11]. The proximal tubule has enormous levels of AQP1 expression. It can carry O_2 to extracellular space, thence, decrease the production of intracellular ROS and the mitochondrial disruption to prevent cellular harm[7]. Conversely, AQP2 is most abundant in collecting ducts, which are vital in modulating fluid volume and urine concentration[10,43]. Besides the impacting proximal tubule function, also, Cr has been associated with collecting duct malfunction, as displayed by decrease in AQP2 expression level in the present study. According to some reports, AQPs expression are highly associated to acute renal damage and are useful for its early diagnosis[42]. Our result are in align with study done by Fan et al.[44], that reveal, a decrease in urine volume was downregulate the expression of renal AQP1 and AQP2, with AQP2 downregulation being linked to a reduction in the glomerular filtration rate. Candan et al. revealed that proximal tubule injury was associated with downregulation of AQP1 levels[11]. These results align with our histological analysis, which revealed dramatic proximal tubule damage and a reduction in AQP1 expression in the cortex.

Additionally, kidney tubular damage biomarkers, such as KIM-1, a transmembrane glycoprotein that is noticeably overexpressed in the proximal convoluted tubule epithelial lining during kidney injury[7,45], were significantly elevated in Cr-intoxicated rats in the current study. The expression of KIM-1 was positively correlated with the extent of tubular epithelial damage and creatinine level as confirmed by our hunter correlation coefficient. Damage to the proximal tubule impairs tubular reabsorption, which raises urea and

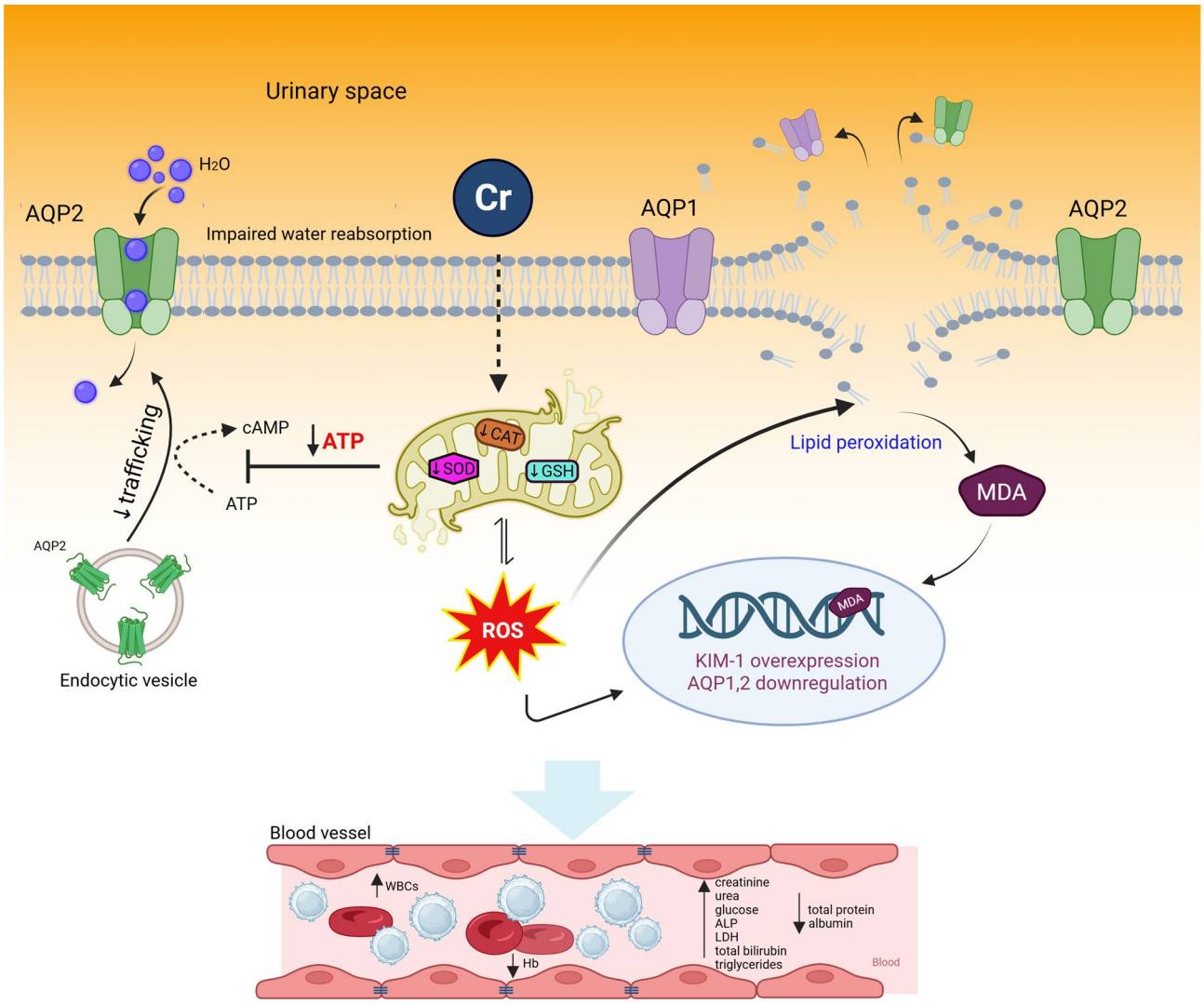

Fig. 11. Proposed molecular mechanisms of potassium dichromate (Cr)-induced nephrotoxicity.

creatinine levels in the blood[46]. These findings corroborate our previous research, Zhang et al. who reported that KIM-1 considerably higher in Cr-intoxicated rats confront to control kidneys. The primary target of renal injury caused by Cr is the proximal tubule. Urinary KIM-1 is a sensitive nephrotoxic biomarker in rats treated with Cr, according to previous laboratory studies[47].

The above-mentioned findings are further supported a significant dose-dependent accumulation of Cr in renal tissues. Thereby, the elevated renal Cr burden correlates well with the observed biochemical changes, oxidative stress, histopathological damage, and dysregulation of AQP1, AQP2, and KIM-1 expressions in this model, supporting the hypothesis that Cr accumulation plays a major role in nephrotoxicity.

In addition to the conventional single-variate analysis, we employed supervised PCA to investigate the dose-dependent manner of Cr treatments on the renal tissue of rats. The PCA biplot clearly demonstrates the differential biochemical and molecular signatures of each group, supporting the conclusion that Cr exposure induces marked oxidative and inflammatory renal injury with Cr-High-intoxicated group notably distinguished out from the other groups. Additionally, Cr-High-induced group are positively associated with classical markers of oxidative stress and renal injury. Furthermore, disruption of KIM-1, AQP1, and AQP2's gene expression in renal membrane shows the strongest correlation with creatinine level, reinforcing their role as a sensitive marker of tubular damage and reflect impaired tubular water handling as elucidated by our hunter correlation coefficient. Similarly, creatinine levels correlations with oxidative stress markers such as MDA, together with ALP and LDH indicating that enhanced LPO, oxidative load, cellular damage and membrane leakage in the kidney tissue following Cr-High exposure. Our findings align with research of Liu et al. who elucidated crucial role of oxidative stress in mediating AQPs downregulation[49]. Serum albumin and total protein also correlated negatively with creatinine, which aligns with the reduced synthetic capacity and altered protein metabolism commonly observed during renal impairment. Cr toxicity cause decrease in protein synthesis or enhance degradation or proteolytic activity and may be because to the detrimental effects of its active metabolite[50]. Furthermore, current VIP score exhibited WBCs count was the most important parameters distinguish the Cr-High-exposed

group from other groups confirming the inflammatory changes upon Cr intoxication as elucidated by our histoarchitecture investigation. On the other hand, it displays AQP1-mRNA expression is the most promising renal marker for Cr intoxication. AQP1 plays a critical role in the modulation of inflammation by inhibiting the leakage of the inflammatory cells, release the inflammatory factors and pseudopodium creation[51]. Consequence, it serve as an excellent biomarker for inflammation[52]. Voslcano plot also revealed Cr-High exposure produced a severe nephrotoxic profile, distinctly different from controls and far more pronounced than the Cr-Low group. Together, these multivariate analyses consistently demonstrate that combined behavior of these biomarkers distinctly separates Cr-High from control and Cr-Low groups, confirming their relevance in describing the progression of renal dysfunction. Figure 11 concludes the molecular mechanisms underlying the toxic effects of Cr on renal tissue.

However, our biochemical markers, molecular findings, histopathological evidence, and ultrastructural observations collectively provide robust indirect evidence of PCT/DCT dysfunction and basement membrane disruption. One limitation of the present study is the absence of direct urine analysis, including mainly measuring the urine volume and osmolality.

Conclusions

Cr clearly provoke notable nephrotoxic effects in a dose-dependent manner through oxidative injury, alteration in the antioxidant defense system, and inflammation. It is important to note that the present study demonstrates that Cr accumulates significantly in renal tissues, confirming the kidney as a primary organ of Cr toxicity. As a result of this bioaccumulation, there is a direct mechanistic link between Cr exposure and the observed biochemical, oxidative, and molecular changes. Overall, our findings highlight that Cr-induced nephrotoxicity is strongly associated with its renal accumulation and subsequent impairment of tubular function and water transport mechanisms. These results further support the use of KIM-1, AQP1, and AQP2 as sensitive biomarkers for early detection of Cr-induced renal injury and emphasize the importance of limiting environmental and occupational exposure to Cr.

Data availability

The datasets generated during and/or analyzed during the current study are available from the corresponding author upon reasonable request.

Received: 8 March 2026; Accepted: 12 May 2026
Published online: 22 June 2026

References

1. Sharma, P., Singh, S. P., Tripathi, R. D. & Tong, Y. W. Chromium toxicity and tolerance mechanisms in plants through cross-talk. *Environ. Pollut*. **320**, 121049 (2023).
2. Hamza, M. A., Hassan, M. S., Mousa, R. F. & Majed, M. S. Evaluation of the antioxidant properties of ginseng green nanoparti-cles in protecting male rats against potassium dichromate toxicity. *J. Kerbala Agric. Sci. Issue*. **11**, 42–51 (2024).
3. Khatoon, N. et al. Human health risks assessment of toxic metals via water, food, and soil: A case study of Northern areas (Ghizer and Gilgit) of Pakistan. *Results Eng.* **24**, 103333 (2024).
4. Bhat, M. A. et al. Chromium and plant health: A prospective study of toxicity to remediation and restoration of the environment. *South. Afr. J. Bot.* **162**, 505–518 (2023).
5. Zheng, X. et al. Hexavalent chromium induces renal apoptosis and autophagy via disordering the balance of mitochondrial dynamics in rats. *Ecotoxicol. Environ. Saf.* **204**, 111061 (2020).
6. Zhang, T. et al. Hexavalent Chromium Induces Neurotoxicity by Triggering Mitochondrial Dysfunction and ROS-Mediated Signals. *Neurochem Res.* **49**, 660–669 (2024).
7. Abdelrahaman, D., Shanab, O. & Abdeen, A. Bee venom ameliorates gentamicin-induced kidney injury by restoring renal aquaporins and enhancing antioxidant and anti-in fl ammatory activities in rats. *Front. Pharmacol.* 1–15. https://doi.org/10.3389/fphar.2025.1525529 (2025).
8. Tamma, G. et al. Aquaporin membrane channels in oxidative stress, cell signaling, and aging: Recent advances and research trends. *Oxid. Med. Cell. Longev.* (2018). (2018).
9. Abdeen, A. et al. Acetazolamide enhances the release of urinary exosomal aquaporin-1. *Nephrol. Dial Transpl.* **31**, 1623–1632 (2016).
10. El-Agawy, M. S. E. et al. Methotrexate-Induced Alteration of Renal Aquaporins 1 and 2, Oxidative Stress and Tubular Apoptosis Can Be Attenuated by Omega-3 Fatty Acids Supplementation. *Int J. Mol. Sci* **23**, (2022).
11. Candan, B., Karakuyu, N. F., Gülle, K. & Sarman, E. Ulusoy Karatopuk, D. Beneficial Effects of Selenium on Kidney Injury via Nf-Kb and Aquaporin-1 Levels. *Biol. Trace Elem. Res.* 1–17. https://doi.org/10.1007/s12011-023-03928-1 (2023).
12. Abdeen, A., Sonoda, H., El-Shawarby, R., Takahashi, S. & Ikeda, M. Urinary excretion pattern of exosomal aquaporin-2 in rats that received gentamicin. *Am. J. Physiol. - Ren. Physiol.* **307**, F1227–F1237 (2014).
13. Jiang, F. W. et al. The novel role of the aquaporin water channel in lycopene preventing DEHP-induced renal ionic homeostasis disturbance in mice. *Ecotoxicol. Env Saf.* **226**, 112736 (2021).
14. Abdeen, A. et al. Decreased Excretion of Urinary Exosomal Aquaporin-2 in a Puromycin Aminonucleoside-Induced Nephrotic Syndrome Model. *Int. J. Mol. Sci.* **21**, 1–12 (2020).
15. Barhoma, R. A. E. The role of eugenol in the prevention of chromium-induced acute kidney injury in male albino rats. *Alexandria J. Med.* 54, 711–715 (2018).
16. Karhib, M. M., El-Sayed, R. A. & El-Demerdash, F. M. Nephroprotective role of Echinacea purpurea against potassium dichromate-induced oxidative stress, inflammation, and apoptosis in rats. *Environ. Toxicol.* **37**, 2324–2334 (2022).
17. Arafa, S. S. et al. Flubendiamide provokes oxidative stress, inflammation, miRNAs alteration, and cell cycle deregulation in human prostate epithelial cells : The attenuation impact of synthesized nano-selenium using Trichoderma aureoviride. *Chemosphere* 365, (2024).
18. Hassan, H. M. et al. Radioprotective potential of whey protein against gamma irradiation-induced lingual damage. *Front. Pharmacol.* **14**, 1–16 (2023).
19. Shanab, O. et al. Modulatory mechanisms of copperII-albumin complex toward N-nitrosodiethylamine-induced neurotoxicity in mice via regulating oxidative damage, inflammatory, and apoptotic signaling pathways. *Ecotoxicol. Environ. Saf.* **270**, 115841 (2024).

20. Beder, E., Bakry, H., Abosalem, M., Abdeen, A. & Badawy, S. Ameliorative activity of cinnamon extract (Cinnamomum Cassia) against aluminum oxide nanoparticle (Al 2 O 3 NP) induced hepatic damage. *Benha Vet. Med. J.* **47**, 47–51 (2024).
21. Elsafty, M., Abdeen, A. & Aboubakr, M. Protective effect of allicin and omega-3 against paracetamol induced hepatic toxicity. *Benha Vet. Med. J.* **43**, 26–31 (2022).
22. Arafa, S. S. et al. Acetamiprid elicits oxidative stress, pro-inflammatory response, and cellular proliferation in human bronchial epithelial cells in vitro and in silico: alleviative implications of the mixture of heat-killed Lactobacillus strains. *Environ Sci. Eur* **36**, (2024).
23. Orhan, S. et al. Chlorogenic acid mitigates potassium dichromate-induced acute hepato-nephrotoxicity by attenuating the NF-κB signalling pathway. *Mol. Biol. Rep.* 51, at (2024). https://doi.org/10.1007/s11033-024-09717-w
24. Ahmed, N. et al. Arabic Gum Could Alleviate the Aflatoxin B1-provoked Hepatic Injury in Rat: The Involvement of Oxidative Stress, Inflammatory, and Apoptotic Pathways. *Toxins (Basel)* 14, (2022).
25. Abdeen, A. et al. Microalgae (Chlorella vulgaris) attenuates aflatoxin-associated renal injury. *Front. Pharmacol.* **14**, 1–15 (2023).
26. Allam, A. et al. N-Acetylcysteine Alleviated the Deltamethrin-Induced Oxidative Cascade and Apoptosis in Liver and Kidney Tissues. *Int. J. Environ. Res. Public. Health*. **19**, 1–13 (2022).
27. Fadl, S. E. et al. Ameliorative effect of Spirulina and Saccharomyces cerevisiae against fipronil toxicity in Oreochromis niloticus. *Ecotoxicol. Environ. Saf.* **242**, 113899 (2022).
28. Bashandy, S. A. E., Amin, M. M., Morsy, F. A. & El-Marasy, S. A. Amelioration of the nephrotoxic effect of potassium dichromate by whey protein and/or nigella sativa oil in male albino rats. *J. Appl. Pharm. Sci.* **6**, 44–50 (2016).
29. Mohsen, A. M., Wagdi, M. A. & Salama, A. Rutin loaded bilosomes for enhancing the oral activity and nephroprotective effects of rutin in potassium dichromate induced acute nephrotoxicity in rats. *Sci. Rep.* **14**, 23799 (2024).
30. Chakraborty, R. et al. Mechanism of chromium-induced toxicity in lungs, liver, and kidney and their ameliorative agents. *Biomed. Pharmacother*. **151**, 113119 (2022).
31. Kamila, S., Dey, K. K. & Chattopadhyay, A. Arsenic and Chromium Induced Toxicity on Zebrafish Kidney: Mixture Effects on Oxidative Stress and Involvement of Nrf2-Keap1-ARE, DNA Repair, and Intrinsic Apoptotic Pathways. *J. Appl. Toxicol.* **45**, 387–399 (2024).
32. Abdelnaby, A. et al. The Combination of Tamarindus indica and Coenzyme Q10 can be a Potential Therapy Preference to Attenuate Cadmium-Induced Hepatorenal Injury. *Front. Pharmacol.* **13**, 1–14 (2022).
33. El-Shoura, E. A. M. et al. Reno-protective effect of nicorandil and pentoxifylline against potassium dichromate-induced acute renal injury via modulation p38MAPK/Nrf2/HO-1 and Notch1/TLR4/NF-κB signaling pathways. *J. Trace Elem. Med. Biol.* **85**, 127474 (2024).
34. Momo, C. M. M. et al. Oxidative Effects of Potassium Dichromate on Biochemical, Hematological Characteristics, and Hormonal Levels in Rabbit Doe (Oryctolagus cuniculus). *vetrienary Sci* **6**, (2019).
35. Akinloye, D. I. et al. Acalypha wilkesiana java white restored carbon tetrachloride (CCl 4) -induced reno-hepatic tissue dysfunction in female albino rats. *Clin. Nutr. Open. Sci.* **44**, 66–91 (2022).
36. Awoyomi, O. V. et al. Luteolin mitigates potassium dichromate-induced nephrotoxicity cardiotoxicity and genotoxicity through modulation of Kim-1/Nrf2 signaling pathways. *Environ. Toxicol.* **36**, 2146–2160 (2021).
37. Salama, A., Mostafa, R. & Elgohary, R. Effect of L-carnitine on potassium dichromate-induced nephrotoxicity in rats: Modulation of PI3K/AKT signaling pathway. *Res. Pharm. Sci.* **17**, 153–163 (2022).
38. Ejoh, S. A., Iheagwam, F. N. & Olusola, A. O. Potassium Dichromate-Induced Hepato- and Hematotoxicity in Rats: Nutritive Composition and Ameliorative Role of Acacia nilotica L. Leaf. *Jundishapur J. Nat. Pharm. Prod.* **16**, e104346 (2021).
39. Ray, R. R. Adverse hematological effects of hexavalent chromium: An overview. *Interdiscip Toxicol.* **9**, 55–65 (2016).
40. Adjroud, O. Protective effects of selenium against potassium dichromate-induced hematotoxicity in female and male Wistar albino rats. *Ann. Toxicol. Anal.* **22**, 165–172 (2010).
41. Islam, S. M. M. et al. Acute effects of chromium on hemato-biochemical parameters and morphology of erythrocytes in striped catfish Pangasianodon hypophthalmus. *Toxicol. Rep.* **7**, 664–670 (2020).
42. Guo, X., Kong, Y., Kwon, T. H., Li, C. & Wang, W. Autophagy and regulation of aquaporins in the kidneys. *Kidney Res. Clin. Pract.* **42**, 676–685 (2023).
43. Su, W., Cao, R., Zhang, X. Y. & Guan, Y. Aquaporins in the kidney: Physiology and pathophysiology. *Am. J. Physiol. - Ren. Physiol.* **318**, F193–F203 (2020).
44. Fan, Y. et al. Overexpression of aquaporin 2 in renal tubular epithelial cells alleviates pyroptosis. *Transl Androl. Urol.* **10**, 2340–2350 (2021).
45. Yarijani, Z. M. et al. Amelioration of renal and hepatic function, oxidative stress, inflammation and histopathologic damages by Malva sylvestris extract in gentamicin induced renal toxicity. *Biomed. Pharmacother*. **112**, 108635 (2019).
46. Abdeen, A. et al. The potential antioxidant bioactivity of date palm fruit against gentamicin-mediated hepato-renal injury in male albino rats. *Biomed. Pharmacother.* 143, at (2021). https://doi.org/10.1016/j.biopha.2021.112154
47. Zhang, J. et al. Immunolocalization of Kim-1, RPA-1, and RPA-2 in Kidney of Gentamicin-, Mercury-, or Chromium-Treated Rats: Relationship to Renal Distributions of iNOS and Nitrotyrosine. *Toxicol. Pathol.* **36**, 397–409 (2008).
48. Liu, M. et al. Role of mitochondrial oxidative stress in modulating the expressions of aquaporins in obstructive kidney disease. *Am. J. Physiol. - Ren. Physiol.* **314**, F658–F666 (2018).
49. Liu, M. et al. Role of mitochondrial oxidative stress in modulating the expressions of aquaporins in obstructive kidney disease. *Am. J. Physiol. Ren. Physiol.* **314**, F658–F666 (2018).
50. Abd-Elfatah, M. et al. An Evaluation of Hepatotoxicity, Nephrotoxicity, and Genotoxicity Induced by Acute Toxicity of Hexavalent Chromium and Comparison of the Possible Protective Role of Selenium and Vitamin E on These Effects. *Ain Shams J. Forensic Med. Clin. Toxicol* 48–58 (2019).
51. Liu, C. M. et al. Aquaporin 1 alleviates acute kidney injury via PI3K-mediated macrophage M2 polarization. *Inflamm. Res.* **69**, 509–521 (2020).
52. Li, B. et al. Aquaporin-1 attenuates macrophage-mediated inflammatory responses by inhibiting p38 mitogen-activated protein kinase activation in lipopolysaccharide-induced acute kidney injury. *Inflamm. Res.* **68**, 1035–1047 (2019).

Acknowledgements

The authors extend their appreciation to the Deanship of Scientific Research and Postgraduate at King Khalid University for funding this work through a Large Group Research Project under grant number (RGP2/536/46).

Author contributions

Conceptualization, investigation, and methodology were performed by Hossam Shehab, Ibrahim E Elsayed, Eman A Badr, Afaf Abdelkader, Eman E ELwakeel, Nagah E Ali, Enas M Kasem, Fatma Al-Zahraa Al-Shahed, and Ahmed Abdeen. Formal analysis, data curation, resources, softwares, validation, and visualization were carried out by Nuha Anajirih, Madaniah O Zakari, Ekramy M Elmorsy, Samah F Ibrahim, Mustafa Shukry, Eman M El Nashar, Areej M Alshehri, Ahmad F Rawan, and Ahmed Abdeen. Writing-original draft preparation, review,

and editing were contributed to by all authors. Supervision and project administration were overseen by Ahmed Abdeen. Funding acquisition was secured by Samah F Ibrahim and Mustafa Shukry. All authors have read and approved the published version of the manuscript.

Funding
This research was implemented by Princess Nourah bint Abdulrahman University Researchers Supporting Project number (PNURSP2026R127), Princess Nourah bint Abdulrahman University, Riyadh, Saudi Arabia. This work was supported by the Deanship of Scientific Research, Vice Presidency for Graduate Research, King Faisal University, Saudi Arabia (Grant No. KFU262122). The authors also extend their appreciation to all facilities provided by the Center of Excellence in Screening of Environmental Contaminants (CESEC; STDF grant No. 31290), Benha University and the Central Laboratory, Faculty of Medicine, Menoufia University.

Declarations

Competing interests
The authors declare no competing interests.

Institutional review board statement
All animal procedures strictly adhered to the UK Animals Act. 1986 (ASPA) and the 3Rs principles (replacement, reduction, refinement). The Research Ethical Committee of the Faculty of Veterinary Medicine, Benha University, Egypt, approved the care and use of laboratory animals, and the experimental rats complied with their guidelines (Approval No. BUFVTM 01-06-25).

ARRIVE guidelines statement
This study aligns with the ARRIVE guidelines to ensure rigorous, transparent, and detailed reporting of experimental design, methodologies, and results in animal research.

Additional information
Correspondence and requests for materials should be addressed to M.S., A.F.R. or A.A.